The Astronomical Journal, 141:103 (7pp), 2011 March doi:10.1088/0004-6256/141/3/103

A THERMAL EVOLUTION MODEL OF CENTAUR 10199 CHARIKLO

A. Guilbert-Lepoutre
Department of Earth and Space Sciences, UCLA, Los Angeles, CA 90095, USA; aguilbert@ucla.edu
Received 2010 September 20; accepted 2011 January 11; published 2011 February 11

ABSTRACT

Centaur 10199 Chariklo appears to have a varying spectral behavior. While three different spectral studies detect the presence of water ice at the surface, two more recent studies do not detect any absorption bands. In this article, we consider the possibility that Chariklo undergoes cometary activity that could be responsible for the observed spectral variations. We simulate its thermal evolution, finding that crystalline water ice should be present in the object core, and amorphous water ice should be found at the surface. Upon entering the inner solar system, Chariklo might experience some cometary activity due to ice crystallization if the obliquity is high, due to the adjustment of the internal structure to a new thermal equilibrium. No other activity is expected from this source, unless an external source like an impact provides the heat needed. In the case of such an event, we find that dust emitted in a coma is unlikely to be responsible for the observed spectral variations. In contrast, water ice grains in the coma would reproduce this pattern, meaning that the water ice detected after Chariklo's discovery was present in these grains and not on the object surface. Nonetheless, any activity would require an external additional heat source to be triggered, through an outburst, which might favor the spatial variations hypothesis.

Key words: conduction – Kuiper belt objects: individual (10199 Chariklo) – methods: numerical

Online-only material: color figures

1. INTRODUCTION

Centaur 10199 Chariklo (1997 CU_{26}), discovered by the Spacewatch telescope in 1997 (Scotti 1997), is the largest Centaur known so far, with a diameter estimated to be from 236 to 302 km (Jewitt & Kalas 1998; Altenhoff et al. 2001; Groussin et al. 2004; Stansberry et al. 2008). The orbital elements from the Minor Planet Center are the following: a semimajor axis of 15.8 AU and an eccentricity of 0.17, which give a perihelion and aphelion distance of 13.1 and 18.5 AU, respectively, and an inclination of 23.3 deg. The object rotation period is still unconstrained (Peixinho et al. 2001).

Three independent spectroscopic studies of Chariklo have reported detection of water ice absorption bands located at 1.5 and 2.0 μm (Brown et al. 1998; Brown & Koresko 1998; Dotto et al. 2003; see Figure 1). However, more recent observations obtained with a higher signal-to-noise ratio have shown a different spectral behavior (Guilbert et al. 2009a, 2009b): no absorption band can be detected in the 1.4–2.4 μm region. Consequently, it appears that Chariklo's spectrum is varying, and the 2.0 μm absorption band depth would seem to decrease with time, from 20% $\pm$ 6% for the first spectrum observed by Brown et al. (1998) to 0% $\pm$ 3% for the last spectrum (see Figure 2). No 1.65 μm absorption band, usually used to diagnose the presence of crystalline water ice, has ever been reported.

Guilbert et al. (2009b) tried to interpret the observed spectral variations in terms of possible cometary activity or variations of the composition over the surface. Cometary activity is present in a number of Centaurs at distances rivaling that of Chariklo (Jewitt 2009). They could not constrain the spatial variations of the composition due to the unknown rotational period. No coma could be detected on any of the images available, leading to a lack of constraints on temporal variations too. In this article, we consider the possibility that Chariklo might undergo thermal processes that could trigger cometary activity. By applying a fully three-dimensional thermal evolution model, we would like to understand if temporal variations like cometary activity are likely to produce the different spectra which have been observed over the last decade. The thermal evolution model is described in Section 2, and the results obtained for Chariklo's thermal evolution are presented in Section 3. Section 4 discusses the interpretation of the observational results with respect to the modeling results.

2. THERMAL EVOLUTION CODE

2.1. Equations and Assumptions

To study the thermal evolution of Chariklo, we used a fully three-dimensional model described in Guilbert-Lepoutre et al. (2011). This model aims to evaluate the temperature distribution and evolution taking into account thermal and physical processes including the decay of radioactive nuclides and the crystallization of amorphous water ice. The model assumes that the objects are spheres made of a porous matrix of amorphous and/or crystalline water ice. Dust is homogeneously distributed within this matrix. Neither sublimation nor condensation of volatiles, nor gas flow inside the matrix, are accounted for in the current version of the model. The model thus solves the heat diffusion equation

$$\rho_{\rm bulk} c \frac{\partial T}{\partial t} + \nabla(-\kappa \overrightarrow{\nabla} T) = \mathcal{S}, \quad (1)$$

where T (K) is the temperature distribution to be determined, $\rho_{\rm bulk}$ (kg m^{-3}) is the object's bulk density, c (J kg^{-1} K^{-1}) is the material heat capacity, κ (W m^{-1} K^{-1}) is its effective thermal conductivity, and $\mathcal{S} = \mathcal{Q}_{\rm rad} + \mathcal{Q}_{\rm cryst}$ are the heat sources. The latter corresponds to the heating due to the decay of radiogenic nuclides (see Table 1):

$$\mathcal{Q}_{\rm rad} = \sum_{\rm rad} \rho_d X_{\rm rad} H_{\rm rad} \frac{1}{\tau_{\rm rad}} \exp\left(\frac{-t}{\tau_{\rm rad}}\right), \quad (2)$$

with ρ_d the dust bulk density, $X_{\rm rad}$ the initial mass fraction of a given radioactive isotope, $H_{\rm rad}$ the heat released per unit mass upon decay, and $\tau_{\rm rad}$ its mean lifetime. The object formation

Table 1
Short- and Long-lived Radioactive Isotopes Accounted for in the Model

Nuclide	$X_{rad}(0)$	τ_{rad} (yr)	H_{rad} (J kg^{-1})
^{26}Al	6.7×10^{-7}	1.05×10^{6}	4.84×10^{12}
^{60}Fe	2.5×10^{-7}	2.16×10^{6}	5.04×10^{12}
^{53}Mn	2.8×10^{-8}	5.34×10^{6}	4.55×10^{12}
^{40}K	1.2×10^{-6}	1.80×10^{9}	1.66×10^{12}
^{232}Th	6.0×10^{-8}	2.02×10^{10}	1.68×10^{13}
^{235}U	9.0×10^{-9}	1.02×10^{9}	1.82×10^{13}
^{238}U	2.9×10^{-8}	6.45×10^{9}	1.92×10^{13}

Notes. X_{rad}: initial mass fraction, to be reduced during the formation delay considered; τ_{rad}: mean lifetime; H_{rad}: heat released upon decay per unit mass. Data from Castillo-Rogez et al. (2007, and references therein).

delay (time required for the object to grow to its final size) is accounted for in the model through the decay of radioactive isotopes that occurs during accretion. Decay results in a decrease of each nuclide initial abundance in the simulations:

$$X_{rad}(t_F) = X_{rad}(0)e^{-t_F/\tau_{rad}}, \quad (3)$$

with t_F the formation delay and $X_{rad}(0)$ found in Table 1. The heating due to water ice crystallization is described by

$$\mathcal{Q}_{cryst} = \lambda(T)\rho_a H_{ac}, \quad (4)$$

with ρ_a the amorphous water ice bulk density. The phase transition releases a latent heat $H_{ac} = 9 \times 10^4$ J kg^{-1} (Klinger 1981), with a rate measured by Schmitt et al. (1989) of

$$\lambda(T) = 1.05 \times 10^{13} e^{-5370/T}\ \mathrm{s}^{-1}. \quad (5)$$

Boundary conditions at the surface include several thermal processes.

1. Solar illumination described by $(1-\mathcal{A})\frac{F_\odot}{d_H^2}\cos\xi$, with $\mathcal{A}$ as the Bond albedo, $F_\odot$ as the solar constant, d_H representing the object's heliocentric distance, and ξ indicating the local zenith angle.
2. Thermal emission $\varepsilon\sigma T^4$, with ε as the material emissivity, σ indicating the Stefan–Boltzmann constant, and T representing the temperature.
3. Lateral and radial heat fluxes.

The heat diffusion problem and its boundary conditions are represented in terms of real spherical harmonics, allowing for efficient numerical implementation. Real spherical harmonics offer a simple and natural expression of the temperature over a spherical grid. Guilbert-Lepoutre et al. (2011) describe in detail the expansion of the temperature distribution and boundary conditions, as well as the resolution of the resulting equations.

2.2. Initial Parameters

Modeling the thermal evolution of a trans-Neptunian object (TNO) or a Centaur requires the initialization of parameters defining the object itself, the material of which it is made, and its orbit. Some parameters can be directly derived from observations like the radius and albedo; some others have to be assumed. This is the case for physical parameters related to the material (composition, porosity, heat capacity, thermal conductivity, etc.) since they are difficult to infer from observations. We decomposed the study of Chariklo in two periods, early and late evolution, so as to focus on thermal processes that dominate each period. The thermal process that dominates the early evolution is heating due to the decay of radioactive nuclides, especially short-lived nuclides. Chariklo's late thermal evolution should be dominated by the effects of insolation, although the effects of long-lived radioactive isotopes have to be included. The parameters we used to study Chariklo can be found in Table 2.

Table 2
Initial Values of the Different Parameters Introduced in the Modeling of Chariklo's Thermal Evolution

Parameter	Symbol	Value
Radius	R	130 km
Bond albedo	$\mathcal{A}$	6%
Mass fractions	X_d/X_{H_2O}	1
Porosity	ψ	30%
Bulk density	ρ_{bulk}	1020 kg m^{-3}
Heat capacity	c	7.6×10^2 J kg^{-1} K^{-1}
Thermal conductivity	κ	6×10^{-3} Wm^{-1}K^{-1}
Initial temperature	T_{init}	30 K
Emissivity	ε	0.9
Semimajor axis	a	15.795 AU
Eccentricity	e	0.171
Rotation period	P_{rot}	20 hr

Chariklo dynamical history. As a Centaur, Chariklo has an unstable orbit over the age of the solar system. Tiscareno & Malhotra (2003) suggested that Centaurs originate in the scattered disk; Chariklo might have thus been a scattered disk object (SDO) before becoming a Centaur by gravitational cascade. However, the origin of SDOs is not clearly identified. Levison & Duncan (1997) suggested that they could be a transient population between objects formed in the Kuiper Belt and more external regions. On the other hand, Duncan & Levison (1997) suggested that they could be a relic of the population formed closer to the Sun and then scattered by Neptune during its outward migration. The actual scattered disk could be a superposition of these two populations. Therefore, without any dynamical study of Chariklo, it is extremely hard, if not impossible, to estimate its formation distance and orbit, as well as the SDO orbit Chariklo might have been a part of.

We first assume that Chariklo was formed in the trans-Neptunian region, following Levison & Duncan (1997). This formation stage is not studied in the model. We make the assumption that Chariklo underwent a cold accretion: accretional heating is neglected here by presuming the object formed from smaller planetesimals which cannot retain efficiently the internally produced heat (Prialnik & Podolak 1999). The accumulation of gravitational potential energy is generally assumed to be negligible even for large bodies such as Pluto (McKinnon et al. 1997); it is also neglected here. In other words, we suppose that Chariklo did not suffer from much thermal modification during its formation period. The simulations presented in this paper will focus on the evolution after this formation period, once Chariklo has reached its final size and its scattered disk orbit, using an initial temperature of 30 K. To estimate Chariklo's internal structure evolution while heated by radioactive isotopes decay, we need to perform long-term simulations focused on the interior of the object. The accurate orbit has little importance in such calculations since the heat input from the Sun is not the dominant energy source for this period of the evolution. We thus assume that Chariklo was placed on an orbit with a semimajor axis of 60 AU and an eccentricity of 0.5.

Table 3
Chariklo's Photometric Properties

Reference	Date	V	R (AU)	Δ (AU)	α	$V(1,1,0)$
Davies et al. (1998)	1997 May	18.47 ± 0.03	13.86	14.02	4.10	6.66 ± 0.03
Peixinho et al. (2001)	1999 Mar	18.02 ± 0.07	13.49	12.73	2.80	6.59 ± 0.07
Peixinho et al. (2001)	1999 Apr	18.02 ± 0.07	13.48	13.06	3.95	6.46 ± 0.07
Peixinho et al. (2001)	2000 Feb	18.04 ± 0.03	13.36	12.43	1.48	6.81 ± 0.03
Bauer et al. (2003)	2000 Feb	18.08 ± 0.02	13.36	12.41	1.28	6.87 ± 0.02
Bauer et al. (2003)	2000 Dec	18.30 ± 0.01	13.25	12.91	4.05	6.77 ± 0.01
Bauer et al. (2003)	2001 Oct	18.42 ± 0.02	13.16	13.75	3.41	6.83 ± 0.02
Bauer et al. (2003)	2002 Jan	18.30 ± 0.02	13.15	12.52	3.40	6.91 ± 0.02
DeMeo et al. (2009)	2007 Mar	18.49 ± 0.05	13.28	12.50	2.75	7.14 ± 0.05
Guilbert et al. (2009b)	2008 Feb	18.79 ± 0.02	13.40	13.32	4.22	7.15 ± 0.02

Notes. V: observed V magnitude; R and Δ: heliocentric and geocentric distances, respectively, at the time of observations; α: phase angle; $V(1,1,0)$: V-band absolute magnitude, computed using $\beta = 0.09$ (Bauer et al. 2003) for Centaurs.

The body and material. Durda & Stern (2000) showed that objects larger than 100 km should not be significantly altered by the collisions they suffered during their life. For the two phases of the evolution—early and late—we thus assume that the size of Chariklo has not changed. We used the values given by Stansberry et al. (2008) for the size (Table 2). The rotation period is still unknown; Davies et al. (1998) reported no clear variable periodic signal, but since they had only a few observations within three days, they argued that a period might exist, which should be very long or close to 24 hr. Peixinho et al. (2001) detected a weak period at 18.5 hr in their R-band data, but below the 50% confidence level, and absent from the V-band data. The study indicates that the rotation of Chariklo should be slow, so we choose a rotation period of 20 hr for the simulations.

Chariklo's surface composition should not reflect its internal composition. Indeed, the surfaces of icy bodies suffer from substantial alteration over the age of the solar system, due to the space weathering processes. We thus have to assume a composition: we chose a mass fraction ratio between water ice and dust of 1, which is directly related to the object density (about 1 g cm^{-1}) and porosity (30%). The water ice is assumed to be initially amorphous. The thermal conductivity and heat capacity are then computed using these values following the formulae presented in Guilbert-Lepoutre et al. (2011). Table 2 gives the initial values for these parameters.

3. RESULTS

3.1. Effect of Short-lived Isotopes

The formation time is a critical parameter since the amount of nuclide available for heating the body is directly related to it. This parameter is, however, not yet fully constrained for TNOs and Centaurs. Nonetheless, Weidenschilling (2004) suggested that objects with a 50 km radius could be formed within 30 AU in less than a million years (Myr), and Kenyon et al. (2008) estimated that in the 20–25 AU region, it would take 5–10 Myr to form 100 km radius objects.

Several formation delays have been tested to estimate the influence of this parameter on Chariklo's thermal evolution (Figure 3). Although the case of a 0.0 Myr formation delay has no physical meaning, we show it as a constraint on the maximum temperature which can be achieved on the internal parts of Chariklo. The crystallization threshold is reached for all the delays presented in Figure 3 after a few million years (it is achieved after 70 Myr when we consider a formation delay of 2.0 Myr). Beyond a formation time of 2.0 Myr, the temperature inside the body is not high enough to allow for the amorphous water ice to crystallize due to heating by short-lived nuclide decay.

As a consequence, for formation delays larger than 2.0 Myr, the internal structure of Chariklo is almost pristine: the temperatures achieved can nonetheless allow for the sublimation of any frozen volatiles. For formation delays smaller than 2.0 Myr, we find that Chariklo suffers from chemical differentiation. A crystallization front rapidly propagates toward the surface: volatiles trapped in the amorphous ice are thus released. The high temperatures reached in the internal parts of the body also induce the sublimation of frozen volatiles. The gas can then flow through the porous matrix toward colder regions close to the surface, or eventually escape from the body, as suggested by Choi et al. (2002) and Prialnik et al. (2008). A layer of amorphous ice is maintained at the surface of Chariklo. Our simulations show that the thickness of this layer ranges from a few hundreds of meters, for the smallest formation delays, to a few kilometers. For the delay of 0.5 Myr, the depth of the first layer fully crystallized is about 380 m, although crystalline water ice can be found locally 100 m under the surface. For the 1.5 Myr delay, crystalline water ice can be found locally at depths below 2 km; the first fully crystallized layers are located at 18 km under the surface.

3.2. Effect of Long-lived Isotopes

The influence of long-lived nuclide decay does not strongly depend on the object formation time, unlike the influence of short-lived nuclides decay. This means that whatever the modification due to early heating is, the internal structure can be further affected by the heating due to long-lived radionuclides.

Our simulations over the age of the solar system show that Chariklo's internal structure is indeed modified, the crystallization threshold being achieved within most of the body (see the evolution of the internal temperature in Figure 4). Amorphous water ice is maintained at the surface, the first layer containing crystalline water ice locally is encountered about 800 m deep, the first fully crystallized layer is found about 15 km deep. Substantial chemical differentiation can also be expected. If we take into account the combined effects of short- and long-period radionuclides, the presence of liquid water would require that Chariklo was formed in less than 500,000 years. Radiogenic heating alone (both from short- and long-lived nuclides) is therefore not sufficient to allow for the presence of a liquid phase, unless salts or other compounds like ammonia are present to lower the material melting point.

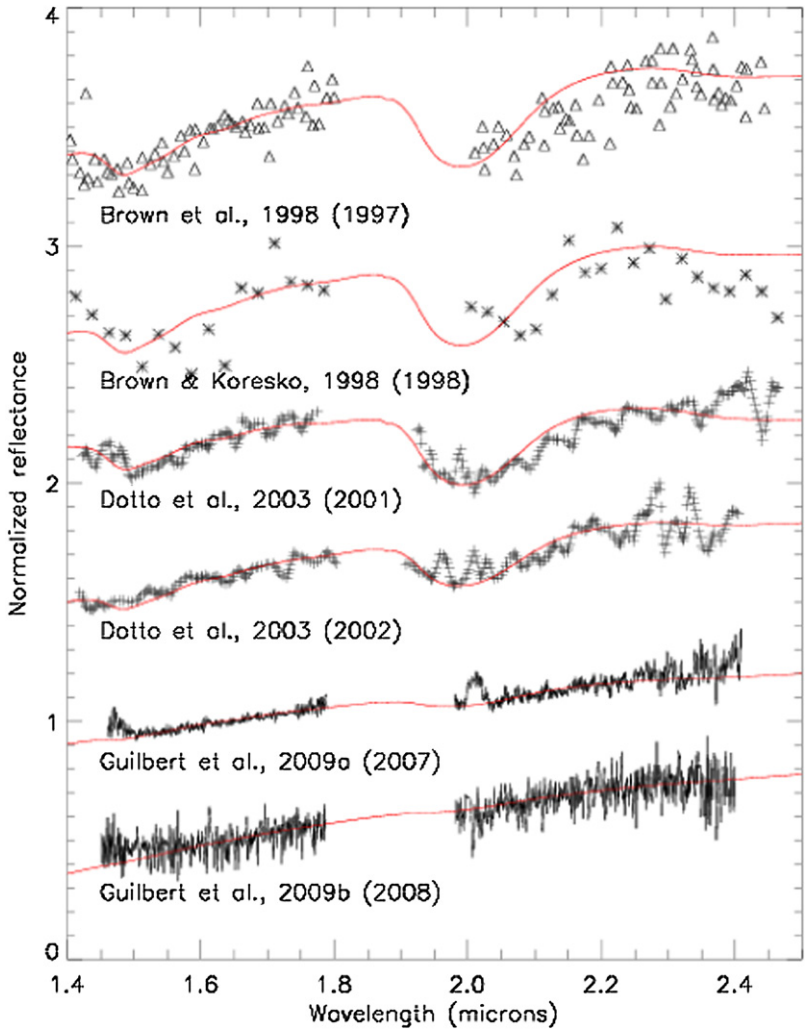

Figure 1. H+K spectra of Chariklo observed by different groups at different times (year in brackets). A synthetic spectrum of water ice (Mastrapa et al. 2008) diluted in some neutral absorber is overplotted on each spectrum to guide the eye. Figure originally published in Guilbert et al. (2009b); reproduced with permission.
(A color version of this figure is available in the online journal.)

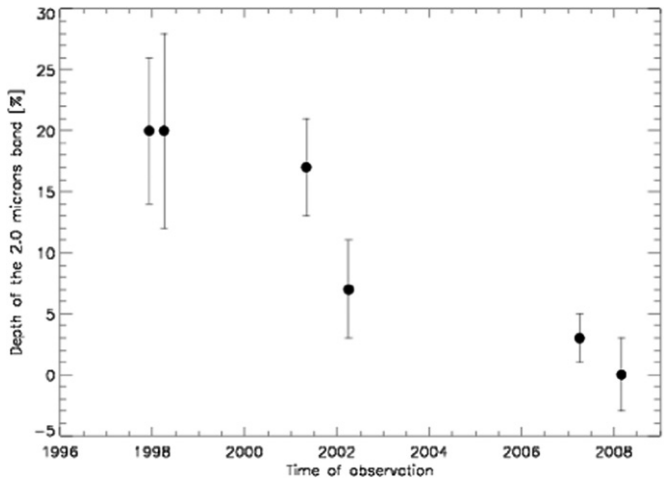

Figure 2. Depth of the 2.0 μm absorption band due to water ice for the different spectra available. Data from Guilbert et al. (2009b).

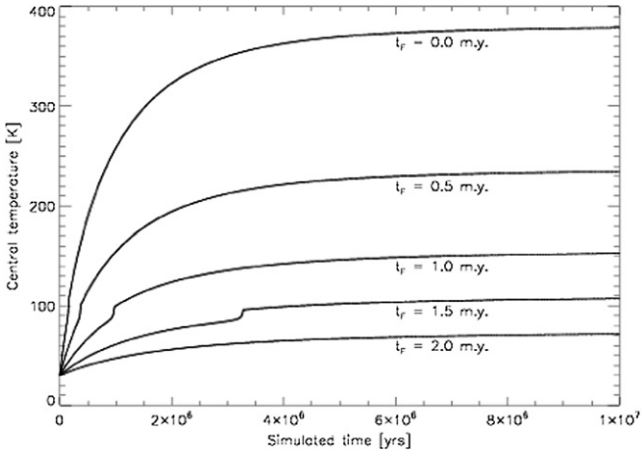

Figure 3. Evolution of Chariklo central temperature as a function of the simulated time (not accounting for the actual formation time t_F which should be added to get the real age of the body). Various formation delays t_F are tested. The temperature jump observed in the curves is due to the heat released upon crystallization of the amorphous water ice.

As a consequence, we find that if Chariklo formed in less than 1.5 Myr, its internal structure results from the influence of short-lived radiogenic nuclides. Otherwise, the internal structure results from the effect of long-lived radiogenic nuclides. In both cases, crystalline water ice can be found relatively close to the surface (few hundred meters to about 1 km), although fully crystallized layers can be located very deep (about 15 km with

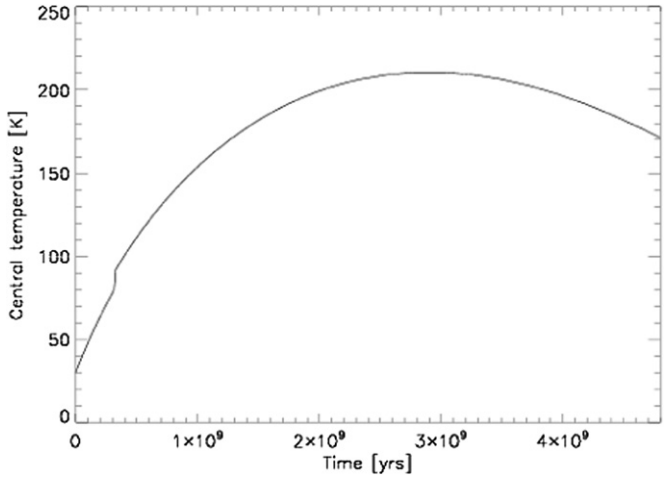

Figure 4. Evolution of Chariklo's central temperature under the influence of long-lived isotopes' radiogenic heating. The temperature jump observed in the curve is due to the heat released upon crystallization of the amorphous water ice.

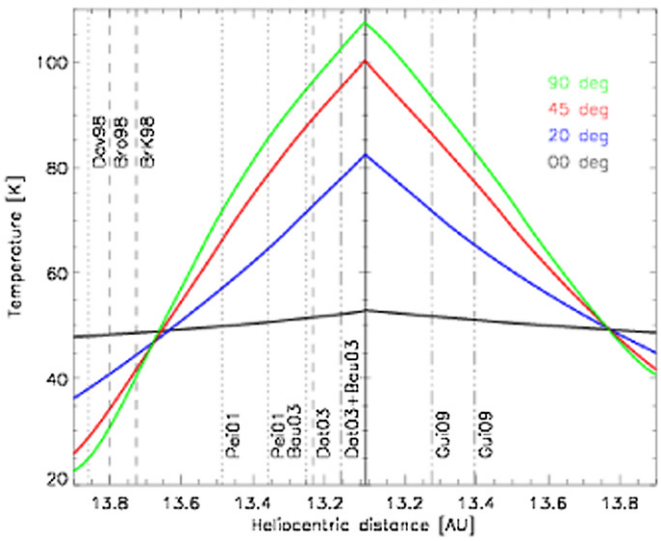

Figure 5. Temperature evolution of the pole facing the Sun when Chariklo orbits around perihelion, as a function of the heliocentric distance, for different obliquities (different curves). The heliocentric distance range we consider here corresponds to the range for the various observations from 1997 to 2008. Vertical lines indicate the position of Chariklo for different observing times: dashes = spectroscopy, dots = photometry, and dot dashes = photometry and spectroscopy. Bau03: Bauer et al. (2003); Bro98: Brown et al. (1998); BrK98: Brown & Koresko (1998); Dav98: Davies et al. (1998); Dot03: Dotto et al. (2003); Gui09: Guilbert et al. (2009b); Pei01: Peixinho et al. (2001).

(A color version of this figure is available in the online journal.)

long-lived nuclides). Erosion by impacts could thus reveal the presence of crystalline water ice only if Chariklo suffered from important cratering. When considering amorphous water ice in the initial composition for the various simulations, we find that amorphous water ice should be the dominant component at the surface. However, Chariklo could have been formed in a region closer to the Sun, where crystallization could be triggered at the surface by insolation.

3.3. Effect of Insolation

Tiscareno & Malhotra (2003) showed that the average lifetime of an object on a Centaur orbit is 9 Myr, although some orbits can be stable for as long as 100 Myr. Horner et al. (2004) suggested that Chariklo's half-life as a Centaur is about 10 Myr. We performed the simulations for 10 Myr on the Centaur orbit. We assume a pristine composition for the surface layer (e.g., a mixture of amorphous water ice and dust), as suggested by simulations presented previously. The temperature distribution and evolution has been studied for different values of the object obliquity (see Figure 5).

Small obliquities. Our simulations show that the surface never achieves the threshold temperature needed to trigger the crystallization of amorphous ice for small values of the obliquity. In the extreme case of an object with an obliquity of 0 deg (poles axis perpendicular to the orbit plane), the maximum temperature at the equator is about 87 K for the whole simulation (from 70 ± 2 K at aphelion to 83 ± 4 K at perihelion, the errors actually being day–night variations).

Large obliquities. The largest equatorial temperature decreases with obliquity, while the maximal temperature in the polar regions increases with obliquity. The simulations show that crystallization of amorphous ice could indeed be triggered at the surface for high obliquities. In the extreme case of a value of 90 deg, the pole facing the Sun at perihelion (the north pole in our simulations) is warmed to almost 110 K. The temperature threshold is actually achieved for co-latitudes smaller than 45 deg, which corresponds to about 15% of the surface. However, crystallization is a temperature-dependent process. It does not have the same efficiency everywhere. In particular, the whole polar cap which achieves the temperature threshold does not fully crystallize: both amorphous and crystalline water ice co-exist. We find that up to 10% of the surface could actually be fully crystallized. Crystallization can induce cometary activity, due to the release of gas trapped in the amorphous ice matrix. Nonetheless, this phenomenon only happens during the first revolutions of Chariklo on its Centaur orbit.

Propagation of the crystallization front. Our results show that crystallization propagates inward following the heat wave penetration inside the body. However, as the object moves from perihelion to aphelion, the surface polar temperature rapidly decreases: the heat wave stops propagating. The crystallization front thus stops propagating, since the local temperature is not increased enough so to reach the threshold. As a consequence, crystallization is possible for a polar cap of a few meters thick only, and the amorphous–crystalline boundary moves a few meters below the surface. Since the boundary has moved deeper, the following heat waves originating at the surface are too weak when they reach this boundary to trigger the crystallization of amorphous ice. The process is thus completely stopped after few orbits; no more activity due to crystallization is expected unless an additional heat input is provided to the body.

4. DISCUSSION

4.1. Internal Structure and Surface Composition

Results on the early evolution of Chariklo show that it is unlikely this object suffered from a physical differentiation including partial melting of the material. However, our simulations show that it did suffer from a chemical differentiation, due to the crystallization of a substantial volume of amorphous ice, under the influence of long-lived radioctive nuclides. If formed in less than 1.5 Myr, this differentiation would be even more important due to the heating by short-lived radioactive nuclides. The crystallization of amorphous ice can induce the release of gas trapped within the matrix. The temperatures achieved in

the internal parts can also allow for the sublimation of volatile compounds present as ices, if any exist.

A layer of amorphous ice is maintained at the surface: its depth depends on the formation delays considered, but ranges from a few hundred meters to a few kilometers. Nonetheless, these results strongly depend on the composition we chose for the simulations: a more ice-rich composition would induce less differentiation, whereas a more rock-rich composition would allow for even more differentiation. Insights into the density of Chariklo are needed to obtain more accurate results on its early thermal evolution. However, an important result is that amorphous ice is probably still present at the surface after this early evolution and below, but the thickness of the amorphous layer would vary from case to case.

We simulated Chariklo's evolution as a Centaur by considering a composition of amorphous water ice and various obliquities. For low values of the obliquity, the crystallization temperature threshold is never achieved during the 10 Myr of the simulations. For high values of the obliquity, the threshold is reached in the polar region facing the Sun at perihelion. A small fraction of the surface can crystallize though: up to 10% of the surface would be fully crystallized.

4.2. Temporal Variations

Some cometary activity can be expected for Chariklo upon arrival in the inner solar system when the structure adjusts to the new thermal conditions. Nonetheless, it only takes a few orbits for the surface to reach a new thermal equilibrium, and no activity would be expected at the present time. Additional external energy input would be required to allow for any further cometary activity. This event could be an impact, for example, which would have to happen when the body is close to the perihelion to efficiently trigger an outburst, since the surface temperatures are close enough from the crystallization threshold. In the case of such an event, would cometary activity be likely to produce the observed spectral variations?

Dusty coma. In the case of Centaur 2060 Chiron, the variations in the spectral behavior and light curve can be explained by the presence of an optically thin coma which dilutes the signal coming from the nucleus. The detection of absorption bands are variable and directly correlated to the object level of activity (Luu et al. 2000; Romon-Martin et al. 2003). In the case of Chariklo, this might seem coherent since activity would be triggered close to the perihelion, where the temperatures are higher.

The emission of dust with sublimating volatiles after its passage at perihelion in 2004 would hide the water ice on the surface, producing the featureless spectra observed by Guilbert et al. (2009a, 2009b). We would expect to observe a coma at the time the level of activity is highest, which would correspond to the observations made by Guilbert et al. (2009a, 2009b). They could not detect a coma on any image available. Moreover, this kind of activity would be likely to produce an increase of the object's overall brightness. This does not correspond to what is actually observed (see Table 3) since the brightness seems to decrease. As a consequence, we believe that the spectral behavior of Chariklo cannot be explained by the presence of any dusty coma.

Icy coma. We could imagine a case where the water ice observed in the spectra is not on the surface of Chariklo, but rather on icy grains emitted after an outburst. Such icy grains containing water ice have already been observed for several comets: C/1995 O1 Hale–Bopp (Davies et al. 1997), C/2002 T7 LINEAR (Kawakita et al. 2004) due to the presence of absorption bands at 1.5 and 2.0 μm in the comae spectra, and 17P/Holmes (Yang et al. 2009) due to bands at 2.0 and 3.0 μm in the coma spectrum. If icy grains were emitted after an outburst in the case of Chariklo, would they survive long enough to be detected?

Grain lifetimes are limited by two main processes: sublimation and sputtering by solar particles. The latter is dominant beyond 7–8 AU (Mukai & Schwehm 1981; Mukai 1986). At Chariklo's smallest heliocentric distance, 10 μm grains (size assumed from spectral modeling results; see Guilbert et al. 2009b and references therein) made of pure water ice could survive 10^{12} s before being destroyed by sputtering (Mukai & Schwehm 1981). Nonetheless, this period would be considerably reduced when considering dusty grains, for which the heating is much more efficient.

If icy grains were emitted during an outburst and then detected in spectra of the object, we would also expect the brightness to be higher when water ice is detected. This is actually the case for Chariklo: the brightness is larger during the period when water ice is detected, whereas it is smaller when no water ice can be observed. Therefore, we believe that if an outburst was triggered close to perihelion and icy grains were emitted, this could be a plausible source of temporal variations to explain the different spectra observed over the time.

4.3. Spatial Variations

Large variations of the composition over the surface could induce the observed spectral variations. This would be likely to produce a detectable light curve; however, this is not observed: V magnitudes and $V-R$ colors published by various authors are all consistent within the error bars (Davies et al. 1998; McBride et al. 1999; Peixinho et al. 2001; Bauer et al. 2003; DeMeo et al. 2009; Guilbert et al. 2009b). Nonetheless this might not be an argument against spatial variations of the composition, as illustrated by the case of Centaur 32532 Thereus. This object has a known rotation period, and spectral variations observed by Merlin et al. (2005) and Licandro & Pinilla-Alonso (2005) have been successfully interpreted as due to heterogeneous repartition of water ice over Thereus' surface (Merlin et al. 2007). However, the $V-R$ color of Thereus does not vary (Farnham & Davies 2003), whereas the $R-J$ color does. Therefore, the spatial variations hypothesis for Chariklo cannot be ruled out by the lack of a noticeable light curve in the visible wavelength range, and new observations should be undertaken to constrain this hypothesis.

A way to rule out the temporal variations hypothesis could be to re-observe a spectrum of Chariklo and detect some water ice. Indeed, our results show that cometary activity could be an explanation of Chariklo's spectral behavior only if icy grains are emitted during an outburst, triggered by an impact close to the perihelion, probably before the first photometric observations in 1997. The probability of this event happening a second time is close to zero. If water ice is detected at the surface of Chariklo on new spectra, this favors the possibility for spatial variations instead of temporal variations.

5. CONCLUSION

In this article, we consider the possibility that Chariklo might undergo cometary activity at the present time, since this could be an explanation of its variable spectral behavior. We thus applied a fully three-dimensional thermal evolution model,

so as to constrain its possible internal structure, its surface composition, and its thermal evolution. The main results are the following.

1. Chariklo's internal structure is likely to be chemically differentiated: water ice, initially amorphous in the simulations, suffers from a substantial crystallization in the core. An outer amorphous water ice layer is maintained. Its thickness depends on initial parameters such as the formation delay and the density, but is at least a few kilometers.
2. Cometary activity can be expected upon arrival in the inner solar system, while the structure adjusts to a new thermal equilibrium, only for high values of the obliquity. In this case, crystalline water ice can be produced on the polar region facing the Sun at perihelion. Only 10% of the surface would then be fully crystallized, which is consistent with the non-detection of any 1.65 μm absorption band in the spectra.
3. No cometary activity is expected at the present time, unless an additional external energy input is provided for the body. This could be possible in the case of an impact, which could trigger an outburst if it happened when the object was close to perihelion.
4. In the case where an outburst was triggered, we find that a dusty coma is unlikely to produce the observed spectral variations, whereas an icy coma could: water ice would in this case be detected on the coma, not on Chariklo's surface.
5. Spatial variations are not to be excluded and should be constrained by new observations.

This work was supported by a NASA Herschel grant to David Jewitt. We are thankful to D. Jewitt, A. Delsanti, and F. Merlin for their useful comments and suggestions, and the referee whose comments helped to improve the manuscript.

REFERENCES

Altenhoff, W. J., Menten, K. M., & Bertoldi, F. 2001, A&A, 366, L9
Bauer, J. M., Meech, K. J., Fernández, Y. R., Pittichova, J., Hainaut, O. R., Boehnhardt, H., & Delsanti, A. C. 2003, Icarus, 166, 195
Brown, M. E., & Koresko, C. C. 1998, ApJ, 505, L65
Brown, R. H., Cruikshank, D. P., Pendleton, Y., & Veeder, G. J. 1998, Science, 280, 1430
Castillo-Rogez, J. C., Matson, D. L., Sotin, C., Johnson, T. V., Lunine, J. I., & Thomas, P. C. 2007, Icarus, 190, 179
Choi, Y., Cohen, M., Merk, R., & Prialnik, D. 2002, Icarus, 160, 300
Davies, J. K., McBride, N., Ellison, S. L., Green, S. F., & Ballantyne, D. R. 1998, Icarus, 134, 213
Davies, J. K., Roush, T. L., Cruikshank, D. P., Bartholomew, M. J., Geballe, T. R., Owen, T., & de Bergh, C. 1997, Icarus, 127, 238
DeMeo, F. E., et al. 2009, A&A, 493, 283
Dotto, E., Barucci, M. A., Leyrat, C., Romon, J., de Bergh, C., & Licandro, J. 2003, Icarus, 164, 122
Duncan, M. J., & Levison, H. F. 1997, Science, 276, 1670
Durda, D. D., & Stern, S. A. 2000, Icarus, 145, 220
Farnham, T. L., & Davies, J. K. 2003, Icarus, 164, 418
Groussin, O., Lamy, P., & Jorda, L. 2004, A&A, 413, 1163
Guilbert, A., Alvarez-Candal, A., Merlin, F., Barucci, M. A., Dumas, C., de Bergh, C., & Delsanti, A. 2009a, Icarus, 201, 272
Guilbert, A., et al. 2009b, A&A, 501, 777
Guilbert-Lepoutre, A., Lasue, J., Federico, C., Coradini, A., Orosei, R., & Rosenberg, E. D. 2011, A&A, in press
Horner, J., Evans, N. W., & Bailey, M. E. 2004, MNRAS, 354, 798
Jewitt, D. 2009, AJ, 137, 4296
Jewitt, D., & Kalas, P. 1998, ApJ, 499, 103
Kawakita, H., Watanabe, J., Ootsubo, T., Nakamura, R., Fuse, T., Takato, N., Sasaki, S., & Sasaki, T. 2004, ApJ, 601, 191
Kenyon, S. J., Bromley, B. C., O'Brien, D. P., & Davis, D. R. 2008, in The Solar System Beyond Neptune, Vol. 592, ed. M. A. Barucci, H. Boehnhardt, D. P. Cruikshank, & A. Morbidelli (Tucson, AZ: Univ. Arizona Press), 293
Klinger, J. 1981, Icarus, 47, 320
Levison, H. F., & Duncan, M. J. 1997, Icarus, 127, 13
Licandro, J., & Pinilla-Alonso, N. 2005, ApJ, 630, 93
Luu, J., Jewitt, D., & Trujillo, C. 2000, ApJ, 151
Mastrapa, R. M., Bernstein, M. P., Sandford, S. A., Roush, T. L., Cruikshank, D. P., & Dalle Ore, C. M. 2008, Icarus, 197, 307
McBride, N., Davies, J. K., Green, S. F., & Foster, M. J. 1999, MNRAS, 306, 799
McKinnon, W. B., Simonelli, D. P., & Schubert, G. 1997, in Pluto and Charon, ed. A. Stern & D. J. Tholen (Tucson, AZ: Univ. Arizona Press), 295
Merlin, F., Barucci, M. A., Dotto, E., de Bergh, C., & Lo Curto, G. 2005, A&A, 444, 977
Merlin, F., Guilbert, A., Dumas, C., Barucci, M. A., de Bergh, C., & Vernazza, P. 2007, A&A, 466, 1185
Mukai, T. 1986, A&A, 164, 397
Mukai, T., & Schwehm, G. 1981, A&A, 95, 373
Peixinho, N., Lacerda, P., Ortiz, J. L., Doressoundiram, A., Roos-Serote, M., & Gutiérrez, P. J. 2001, A&A, 371, 753
Prialnik, D., & Podolak, M. 1999, Space Sci. Rev., 90, 169
Prialnik, D., Sarid, G., Rosenberg, E. D., & Merk, R. 2008, Space Sci. Rev., 138, 147
Romon-Martin, J., Delahodde, C., Barucci, M. A., de Bergh, C., & Peixinho, N. 2003, A&A, 400, 369
Schmitt, B., Espinasse, S., Grim, R. J. A., Greenberg, J. M., & Klinger, J. 1989, in ESA SP-302, Physics and Mechanics of Cometary Materials, ed. J. Hunt & T. D. Guyenne (Noordwijk: ESA), 65
Scotti, J. 1997, Minor Planet Circular, D-11
Stansberry, J., Grundy, W., Brown, M., Cruikshank, D., Spencer, J., Trilling, D., & Margot, J.-L. 2008, in The Solar System Beyond Neptune, Vol. 592, ed. M. A. Barucci, H. Boehnhardt, D. P. Cruikshank, & A. Morbidelli (Tucson, AZ: Univ. Arizona Press), 161
Tiscareno, M. S., & Malhotra, R. 2003, AJ, 126, 3122
Weidenschilling, S. J. 2004, in Comets II, Vol. 745, ed. M. C. Festou, H. U. Keller, & H. A. Weaver (Tucson, AZ: Univ. Arizona Press), 97
Yang, B., Jewitt, D., & Bus, S. J. 2009, AJ, 137, 4538